Electronic Supplementary Material (ESI) for Nanoscale.

Supplementary Information

Molecular level nucleation mechanisms of hierarchical MFI and MOR zeolite structures via non-stochastic pathway

Volkan Şahin* [a], Abdulkerim Karabakan [a]

[a]Department of Chemistry, Hacettepe University, Ankara 06800, Turkey.

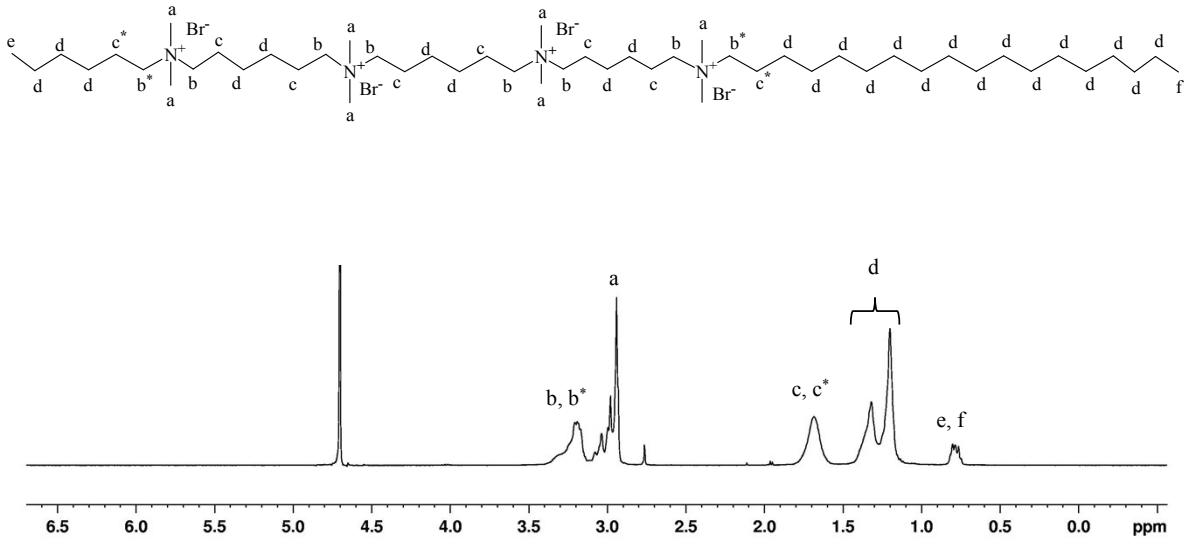

Fig. S1 ^{1}H-NMR spectrum of $C_{6\text{-}666\text{-}18}$ SDA compound was recorded in D_2O solvent using tetramethylsilane standard.

The hydrogen atoms of the molecular structure were characterized by the following chemical shift values in the spectrum, (400 MHz, D_2O), a: 2.94 ppm (24H), b, b*: 3.20 ppm (16H), c, c*: 1.68 ppm (16H), d: 1.15-1.40 ppm (48H), e, f: 0.78 ppm (6H).

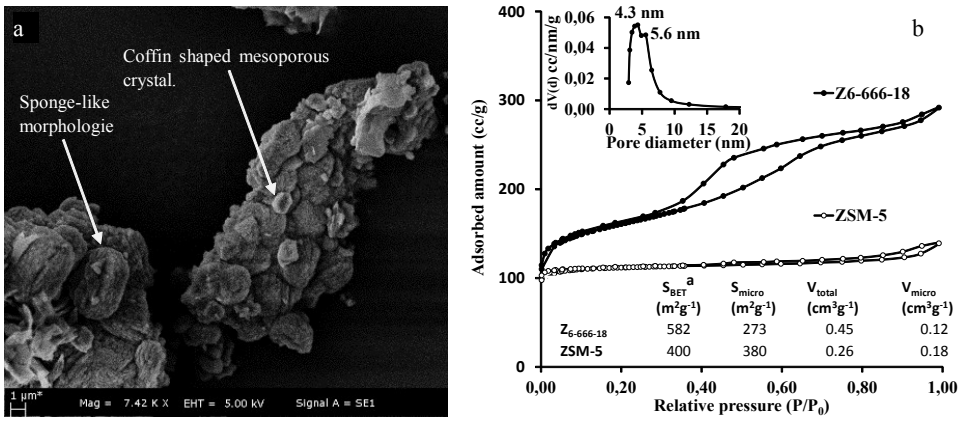

Fig. S2 SEM image (a) of $Z_{6\text{-}666\text{-}18}$ product obtained at the end of reaction period of 10 days, including that three different mesoporous morphologies shown in Figure 1. The N_2 adsorption-desorption isotherm (b) of $Z_{6\text{-}666\text{-}18}$ and conventional ZSM-5 with MFI framework at standard temperature and pressure and the cumulative mesopore size distribution of $Z_{6\text{-}666\text{-}18}$. [a] S_{BET} surface areas of samples were calculated by using N_2 adsorption data on the relative pressure range of 0.015-0.2. $Z_{6\text{-}666\text{-}18}$ presented type IV isotherm which is characteristic for both microporous and mesopore-containing materials due to its hierarchical pore structure. The hystheresis observed in the region of P/P_0 <0.1 in isotherms of ZSM-5 and $Z_{6\text{-}666\text{-}18}$ show N_2 filling to micropores. The second hystheresis within the 0.4-0.8 region in $Z_{6\text{-}666\text{-}18}$ indicates N_2 capillary condensation in mesopores. The pore size distribution of $Z_{6\text{-}666\text{-}18}$ calculated by the BJH method, shows two mesopore types with a diameter of 4.3 nm and 5.6 nm. The non-uniform distribution of the mesopore regime is due to the slightly different mesopore size distribution in the different morphologies identified in this product (Fig.1).

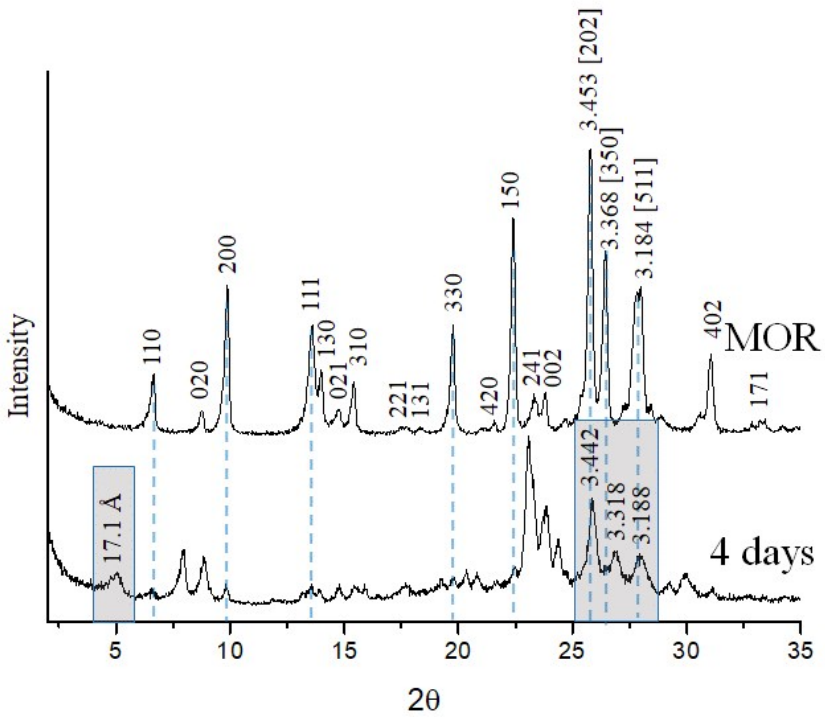

Fig. S3 The diffractions indexed with Miller-indices of MOR framework have been matched with the diffractions of MOR-type content in the 4 days product via blue dashed lines. The diffractions resulted from the high organization state of MPS in the 4 days product have been marked with a gray band. The triple diffraction pattern resulting from high organization state of MPS marked with gray band in the range of 2θ; 25°-29° is very similar to the 'hkl' [202], [350], [511] diffraction pattern of MOR in the same region. The X-ray diffractions resulted from the MOR-type component of 4 days product, have been covered by these MPS diffractions. Their relative intensities (I_{rel}) are very high for MOR framework. All other diffraction signals in the XRD pattern of 4 days product belong to the MFI-type framework.

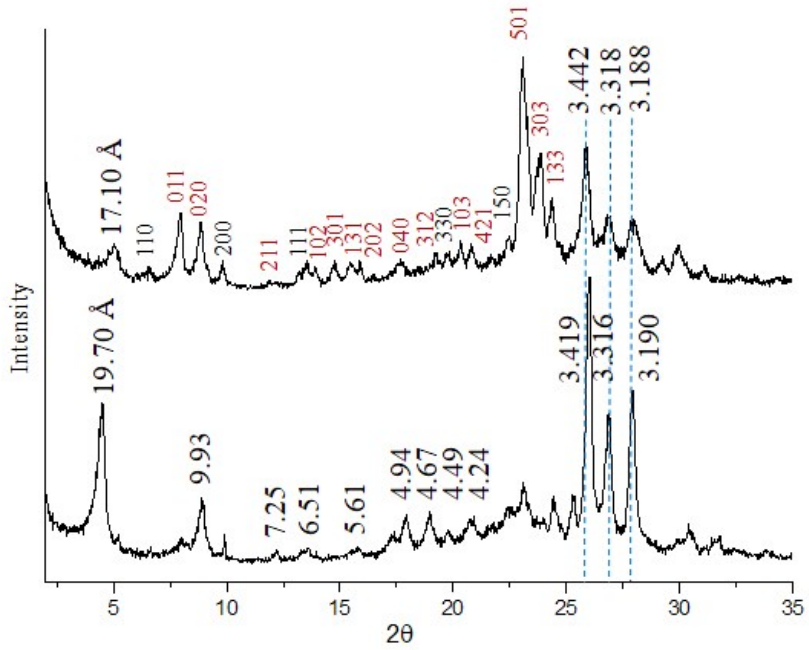

Fig. S4 The XRD patterns for 4 days product of $0Z_{6\text{-}666\text{-}18}$ crystallization period (top), and a unknown silicate product (bottom) obtained by using the template effect of tetraquaternary OSDA under different hydrothermal synthesis conditions from MFI-type $0Z_{6\text{-}666\text{-}18}$ hierarchical zeolite synthesis. The red and black 'hkl' indices in the XRD pattern of the 4 days product belong to the MFI and MOR frameworks, respectively. Three diffraction signals in the X-ray diffractogram of the unknown silicate structure isolated in a high organization state have been matched with the characteristic triple diffraction pattern resulting from the MPS phase in the 4 days product. These diffractions overlap with the diffractions in the same region caused by MFI and MOR phases in 4 days product. This unknown silicate structure also contains same triple diffraction pattern within its full XRD pattern, which is specific to its framework. The XRD pattern of this silicate, except for the triple diffraction pattern, is completely different from the diffraction of the 4 days components. This confirms that MPSs observed with these common diffraction signals can be generated in different organization states with different XRD patterns. The XRD diffractogram of this silicate structure is completely different from that of magadiite except for the diffraction pattern in the same region (2θ; 25°-29°) that is also characteristic for the magadiite mineral.[1,2,3]

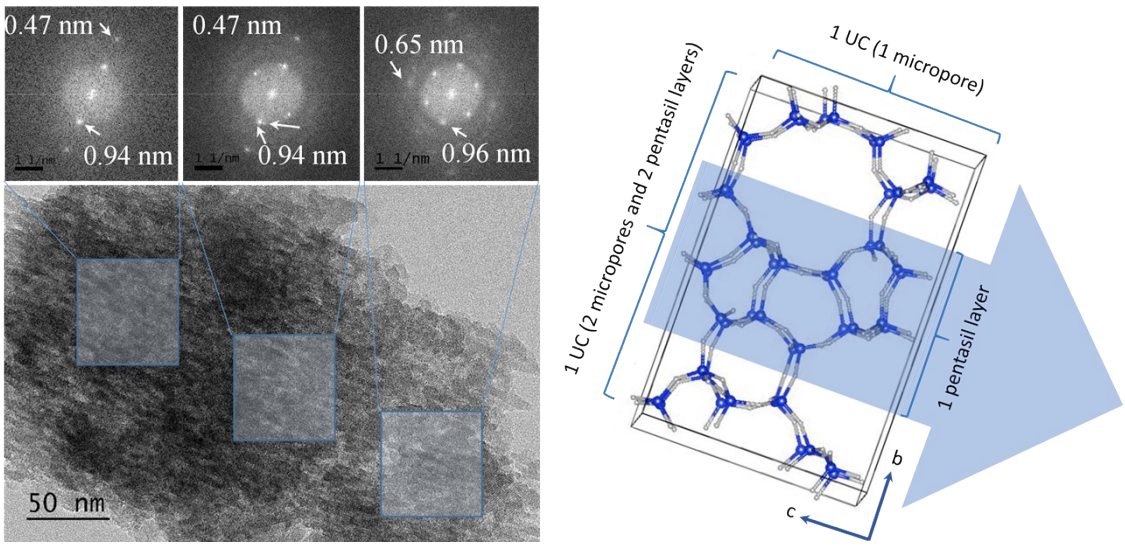

Fig. S5 The HRTEM image belongs to a polycrystalline particle found in 4 days. In the FFT patterns of one-dimensional parallel lines in the micrograph of the particle, 0.94 nm first order and 0.47 nm second order spots are seen. As it progresses along the line giving this pattern on the crystal, new spots have been added to these spots, indicating the formation of lattice regularity in the second dimension. While the 0.94 nm spot disappeared, an 0.96 nm spot at approximately 5° angular distance and an 0.65 nm spots resulting from structural regularity perpendicular to this image regularity appeared. The bc-plane of the MFI unit cell is shown on the image (right). In the figure, the depth in the a-axis has been reduced to half UC. The UC parameters of MFI framework are a: 20.090 Å, b: 19.738 Å, c: 13.142 Å, α: β: ɣ: 90.000° (Orthorombic, Pnma no:62). Values of 0.96 nm and 0.65 nm are suitable for the formation of a pentasil layer thickness (1/2 UC) in the bc-plane of MFI framework. Fourier transform spots of MPS and MFI-type farameworks gradually displaced on the same particle. It is understood that the MPS and MFI structures in this particle are in covalent interaction.

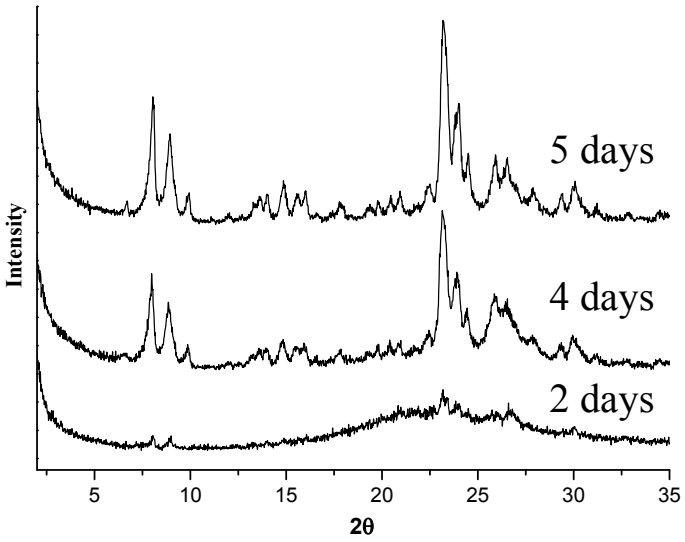

Fig. S6 X-ray diffraction patterns for calcined $Z_{6\text{-}666\text{-}18}$ products which were obtained at hydrothermal reaction time for 2, 4 and 5 days. At the end of the calcination process, the diffraction pattern from the high organization state of MPS in the 2θ; 26°-29° region amorphized, while the diffraction signals in the low angle region of the same structure disappeared.

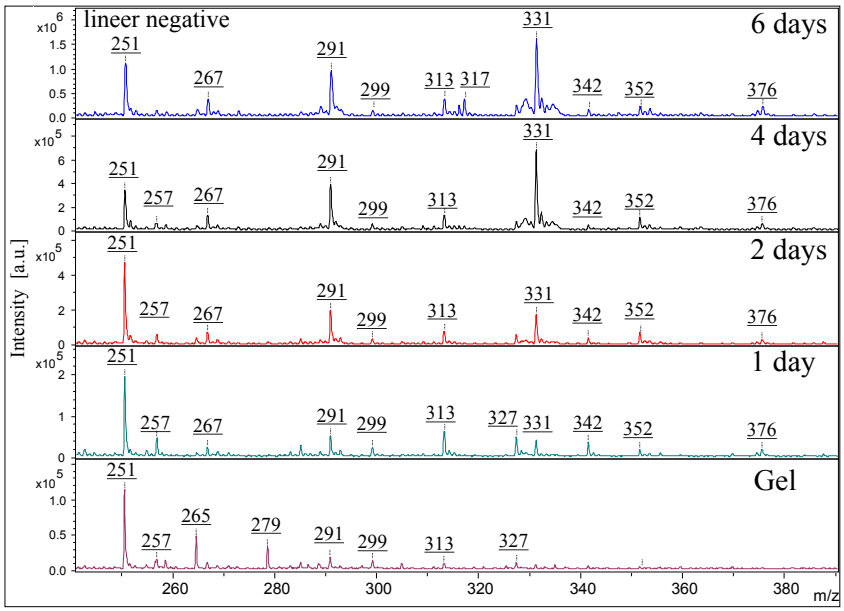

Fig. S7 LDI-TOF MS spectra for gel mixture dried before hydrothermal reaction and as-made products obtained after the hydrothermal reaction time of 1 day, 2 days, 4 days and 6 days. Spectra were collected in lineer negative analysis mode. Since the beginning of the hydrothermal reaction, the ionization efficiency of anionic oligomers with 251, 267, 291, 313, 331, 352 and 376 mass values have increased. During this time period, the Si sites of the low organization degree MPS in the amorphous gel mixture became increasingly specific and the resulting intermediate MPSs crystallized into the MFI-type framework. The oligomer with 251 mass value ionized with the highest yield at 2 days. The relative intensity of the signal of this oligomer to other signals decreased. This indicates that the oligomer with 251 mass value ionized from a MPS in lower organization degree. As seen in main text Fig. 4, this oligomer can be ionized from $MPS_{(A, B)}$.

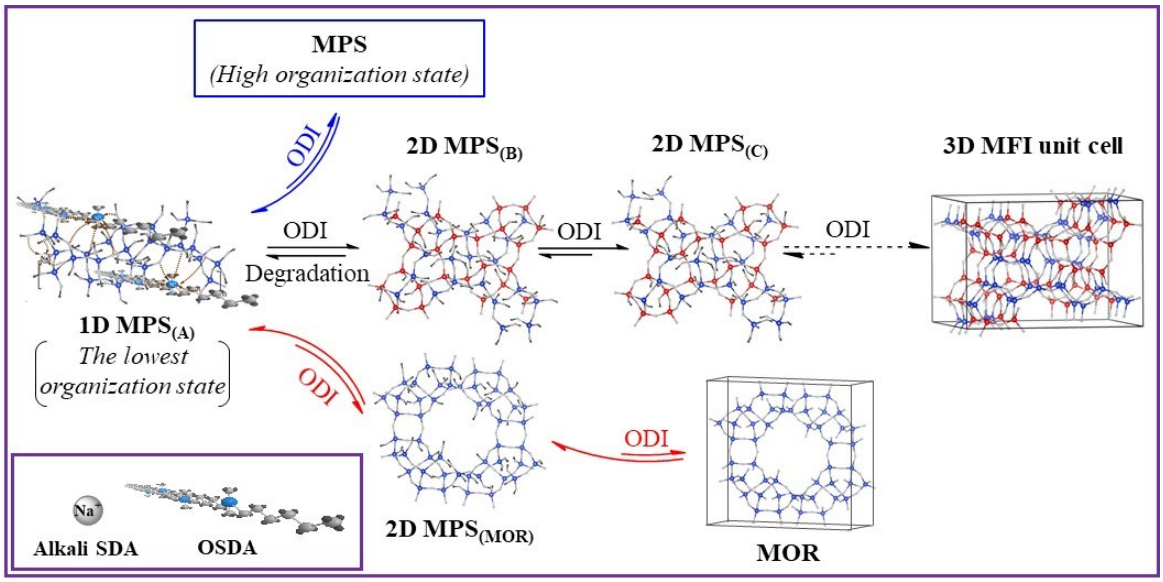

Fig. S8 All products and their intermediates formed during the hydrothermal reaction process of the gel composition, which has been optimized as 1 Al_2O_3: 33 Na_2O: 100 SiO_2: 2,5 $C_{6\text{-}666\text{-}18}$: 3180 H_2O: 7 H_2SO_4: 400 EtOH, were summarized. Since the ODI pathway towards the MFI framework was preferential, all of these species transformed into MFI-type framework at the end of the reaction time. The 1D $MPS_{(A)}$ in the lowest organization degree gradually reached 2D and 3D frameworks via ODI mechanism. The ODI progresses by intra-molecular covalent interactions of 2D MPSs formed by combining the same 1D MPSs. Degradations of the high organization state of MPS and MOR framework, which formed in the same reaction medium, up to the $MPS_{(A)}$ origin are sufficient to their subsequent transformation to MFI framework.

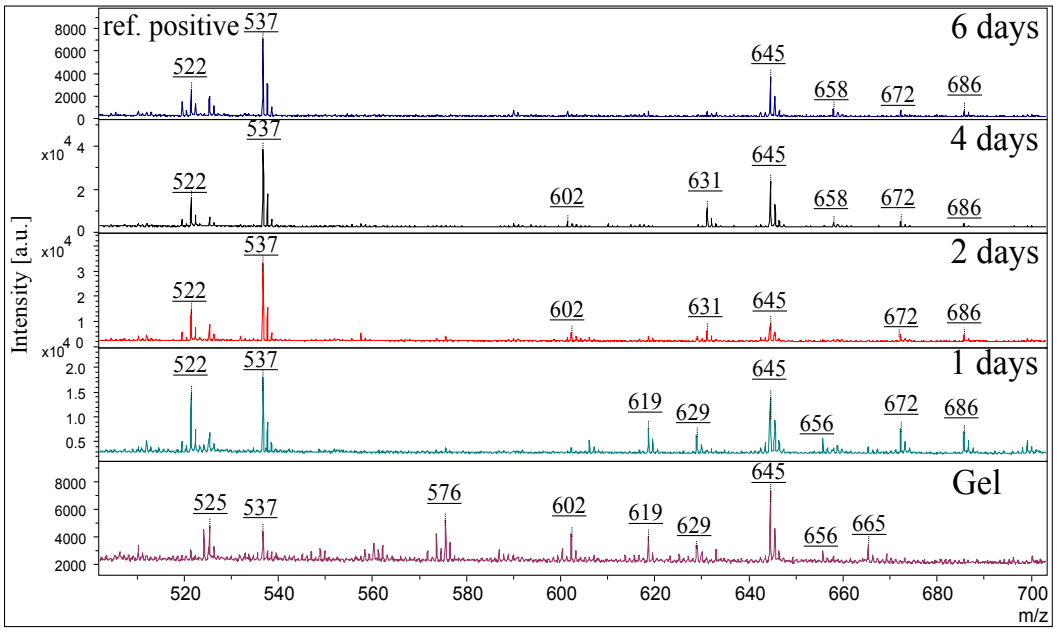

Fig. S9 MALDI-TOF MS spectra for gel mixture dryed before hydrothermal reaction and as-made products obtained after the hydrothermal reaction time of 1 day, 2 days, 4 days and 6 days. Oligomers observed in the mass spectrum of mordenite at m/z 629 and 656, also ionized with low efficiency from dry-gel and in 1 day product.

References

1 Brindley, G. W. Unit Cell of Magadiite In Air, in Vacuo, and Under other Conditions. *The American Mineralogist* 1969, 54, 1583-1591.

2 Blaison, E. C.; Sauzeat, E.; Pelletier, M.; Michot, L. J.; Villieras, F.; Humbert, B. Hydration Mechanisms and Swelling Behavior of Na-Magadiite. *Chem. Mater.* 2001, 13, 1480-1486.

3 Chen, Y.; Yu, G.; Li, F.; Wei, J. Structure and photoluminescence of composite based on ZnO particles inserted in layered magadiite. *Applied Clay Science* 2014, 88–89, 163–169.